Evaluation of Onshore Wind Power Potential to Maximize Renewable Energy-Supported Transportation Electrification – Applied Along the Red Sea Coast of Saudi Arabia

Shahzada Zaman Shuja
Professor
King Fahd University of Petroleum & Minerals (KFUPM), Mechanical Engineering Department
Saudi Arabia

Majid Alotaibi
Master Student
King Fahd University of Petroleum & Minerals (KFUPM), Mechanical Engineering Department
Saudi Arabia

Shafiqur Rehman
Research Engineer
King Fahd University of Petroleum & Minerals (KFUPM), Interdisciplinary Research Center for Sustainable Energy Systems (IRC-SES) and Mechanical Engineering Department
Saudi Arabia

This study evaluates the onshore wind power potential along the Red Sea coast of Saudi Arabia to inform strategic planning for renewable energy-supported transportation electrification. Nine locations, spaced 120-240 km apart, were selected based on 10-year wind speed data and analyzed. Distinct wind patterns were identified between the northwest and southwest coasts. Hourly meteorological data (from January 2014 to December 2023) was obtained and average annual wind speed and power density values were estimated. Sites were evaluated using NREL's classification system. The study utilized the maximum likelihood estimation derived Weibull distribution, shape and scale parameters to model power density and mean speed. Capacity factors were analyzed for 36 wind turbine models spanning 1.5-4MW to identify the wind turbine optimally suited to each region's wind resources. Annual capacity factor performance determined the models' ability to reliably activate concurrent electric vehicle charging ports. Leading choices included Suzlon's 4MW S146 consistently demonstrating highest median port activations. MingYang's 3MW MySE3.0-135 and Windey's 3MW WD140-3000 emerged as optimal with stable double-digit port activations depending on wind resources. SANY's 2MW SE12520 and Windey's 2MW WD121-2000 also performed prominently across sites. Dongfang's 1.5MW G2000-116 maintained strong performance. The results characterize wind energy potential and pinpoint optimal turbine selections capable of stably supporting transportation electrification targets depending on site conditions. In addition, the results also provide valuable information related to strategic integration planning to maximize the onshore wind sector's contribution to Saudi Arabia's renewable energy and emissions reduction goals through electrified transportation.

Keywords: *Wind power, electric vehicle, wind turbine, wind power density, Weibull Distribution*

1. INTRODUCTION

The transition to a greener and more sustainable energy portfolio is imperative for attaining carbon neutrality by 2060. As outlined in the 2014 report published by the Intergovernmental Panel on Climate Change, limiting global warming increases to 1.5°C necessitates average yearly investment of approximately $2.4 trillion in energy efficiency measures, sustainable options, and renewable sources until 2035 [1]. A recent study conducted by McKinsey & Company [2] estimated substantial expenses associated with facilitating this transition. Within a net-zero scenario projected for 2050, cumulative outlays on physical assets are anticipated to reach approximately $275 trillion between 2021 and 2050. Over the past three years, more than 200 GW of wind power capacity has been added globally, indicating a strong and accelerating demand for wind energy [3]. Previously, Europe used to dominate the wind energy market, however, growth in wind power capacity has increasingly been driven by non-European nations. For instance, Saudi Arabia recently commi–ssioned the 400 MW Dumat Al-Jandal wind project and an 850 MW wind farm has been announced in Yanbu on the west coast [4]. These developments demonstrate Saudi Arabia's aim to incorporate greater wind power within the country's energy mix as part of its diversification efforts and transition to renewable sources of energy.

Transitioning to sustainable transportation will also be integral to achieving these climate goals. Electric vehicle (EV) adoption is growing rapidly worldwide due to emissions and fossil fuel dependence concerns. Remote and off-grid areas require innovative renewable energy solutions to enable widespread EV charging access. Achieving carbon neutrality will necessitate a transition to electric transportation on a large scale. As

Received: October 2024, Accepted: December 2024
Correspondence to: Dr Shafiqur Rehman,
King Fahd University of Petroleum & Minerals,
Dhahran, Saudi Arabia.
E-mail: srehman@kfupm.edu.sa
doi: 10.5937/fme2501085S

the proliferation of EVs continues globally, expanding public charging infrastructure is crucial to drive further adoption. Although EVs possess advantages for environmental sustainability and energy security relative to gasoline-powered vehicles, but inadequate infrastructure of charging stations poses a barrier to greater EV usage. Standalone wind-powered charging stations provide an off-grid solution to boost availability while leveraging renewable wind energy. Anxiety due to limited driving range between charges presents one of the key barriers to greater EV uptake. Convenient public charging infrastructure, especially along remote highway locations, can help alleviate these concerns.

Leveraging wind energy will require thorough analysis and modeling of wind resource potential [5-10]. The size and type of turbine selected for wind farms are based on the avalability of wind speed at the chosen sites [11-13]. Wind speed vary significantly due to various factors such as atmospheric conditions, the location, tume of the eyar, height, and land surface roughness. Therefore, it is essential to understand the wind speed characteristics at a prospective site. Several statistical methods have been developed to describe wind speed, including the Weibull, Gamma, Inverse Gaussian, and Exponential distributions. Among these, the Weibull distribution is most widely used [14-20]. The Weibull probability density function can be applied to estimate the variability and magnitude of wind speeds. For example, a study conducted in Johannesburg, South Africa found that the Weibull distribution provided the best fit to the data across all seasons. The study also identified the optimally sized wind turbine for the site and determined that only small, standalone turbines were suitable given the wind resource [14]. Understanding the wind speed distribution is crucial for the selection of an appropriately sized turbine [21-23].

The wind potential of Jeju Island, South Korea was evaluated using data collected over five years at altitudes ranging from 18-513 m across nine locations. Six different Weibull estimation techniques were applied to the dataset: graphical method [GM], power density method [PDM], empirical method of Justus [EMJ], maximum likelihood method [MLM], modified maximum likelihood method [MMLM], and moment method [MM] [24]. The study concluded the graphical method was the least accurate, while the moment method provided the most accurate parameter estimation. Additionally, an assessment of the wind energy potential in Tetouan, northern Morocco employed the Weibull distribution fit to wind speed data measured every 10 minutes at a height of 60 m over three years. Five estimation methods were applied: empirical method of Lysen [EML], MM, EMJ, GM, and PDM. Wind power densities were derived and statistical errors of the distributions were computed. The study found the graphical method to have the greatest error, while the other techniques provided comparable and accurate parameter fits [25].

In Saudi Arabia, researchers analyzed twenty years of wind speed data to estimate the Weibull distribution parameters, including the scale factor proportional to the shape parameter and the average wind speed proportional to the variance, for ten major locations [26]. For example, in the northwest coast region, the city of Tabuk had estimated scale and shape factors of 2.00 and 3.44 m/s, respectively, while Al Wajh, a seaside city located 240 kilometers southeast of Tabuk, had scale and shape factors of 2.50 and 4.83 m/s, respectively. Based on these distribution fits, the wind speeds producing the maximum wind power were calculated to be 6.1 m/s for Al Wajh and 4.9 m/s for Tabuk. In another study, the proposed megacity of Neom, along the northwestern coast, was found to have an average wind speed of 10.3 m/s for power generation according to its Weibull distribution parameters [27].

Given Saudi Arabia's ranking of 13th globally in onshore wind energy production [28], identifying promising wind resource areas across the kingdom to power standalone EV charging stations is strategic. This study assesses 9 coastal locations along the Red Sea: Neom, Duba, Umluj, Yanbu, Rabigh, Jeddah, Al Laith, Al Gunfuthah, and Jazan. These sites were selected to represent diverse geographic regions (Northwest, Midwest, Southwest) and proximity to major population/industry centers. Remote coastal areas require innovative renewable solutions like wind power to enable widespread EV adoption necessary for carbon emissions reductions in transportation sector. This feasibility research evaluates the technical capability of standalone wind-powered fast charging stations as well as suitable wind turbine sizes in the range of 1.5-4.0 MW rated capacities to support electric mobility expansion in the Red Sea region. Wind speed data from 2014-2023, for the selected sites, was obtained from meteorological records. The study will determine the wind energy potential and optimal turbine size required to adequately meet projected vehicle charging station's demands while gaining insight into deploying wind-based infrastructure.

The novelty of the present work lies in the fact that wind power based EV fast charging infrastructure is being proposed along the vast coastal areas of the Red Sea coast of saudi Arabia. To the best of authors understanding, it is first of its kind initiative in Saudi Arabia and the region at large. It is an effort towards the national goal of achieving renewable energy installation in accordance with Kingdom's Vision 2030.

2. SITE SELECTION AND WIND DATA ACQUISITION

Ten-year wind speed data for the selected cities was obtained from the NASA Power Data Access portal [29]. The wind speed data, provided by the NASA Power Project, is collected using ground-based anemometers as well as satellite-based scatterometers. This data is available in hourly intervals at various heights above the ground, enabling analysis of wind resource potential. It is widely utilized for the development and implementation of wind energy systems as well as for studying the impacts of climate change on wind resources. The high spatiotemporal resolution of the NASA Power Data Access wind dataset makes it suitable for assessing long-term wind energy production potential at prospective development sites.

Nine sites, along the west coast of Saudi Arabia, are selected (Figure 1) to examine average wind potential

and seasonal wind patterns. As shown in Table 1, the selected locations are grouped into three regions: Northwest, Midwest, and Southwest. On average, the locations are 12 km inland from the coast, around 180 km apart from each other, and located either near a sizeable city or industrial area. This coastal study region extends from Neom in the north to Jazan in the south. The varying geographic conditions represented across these nine sites provide an opportunity to analyze wind energy feasibility in diverse coastal environments along the Red Sea.

Figure 1. The selected locations along the West Coast of Saudi Arabia

Table 1. Selected locations along the West Coast of Saudi Arabia

Location	Regions	Coordinates (Lat °N Long °E	Elevation (m)	Distance from coast (km)
Neom	Northwest	28.12 34.64	42	2.72
Duba	Northwest	27.15 35.85	59	5.52
Umluj	Northwest	25.52 37.28	191	22.50
Yanbu	Midwest	24.40 37.55	55	9.15
Rabigh	Midwest	23.25 38.80	13	7.65
Jeddah	Midwest	20.98 39.35	45	6.76
Al Laith	Southwest	20.05 40.55	216	9.55
Al Gunfuthah	Southwest	18.56 41.45	45	5.82
Jazan	Southwest	17.50 42.35	25	7.50

3. METHODOLOGY OF WIND ASSESMENT

The 10-year hourly wind speed data is utilized to determine the average annual and monthly wind speeds at each site. The average monthly wind speeds illustrate the seasonal variation across locations. Furthermore, the hourly data was employed to estimate the parameters of the Weibull distribution using the maximum likelihood method. These distribution parameters were then used to calculate the mean wind velocity, most frequent wind speed, maximum power carrying wind speed, and wind power density at the nine sites. Additionally, the 10-year hourly wind data was analyzed to determine the hourly power density. This information played a critical role in evaluating different turbine models to identify the model achieving the highest capacity factor to optimally harness the wind resource potential. Understanding temporal variation in wind speeds and distribution characteristics at each site is vital for feasibility assessment and technology selection for a proposed wind-powered EV charging station. The results of this analysis will be used to determine the suitability of each location for providing adequate renewable energy to power fast charging capabilities for electric vehicles utilizing the station.

3.1 Weibull Distribution

The function of the Weibull distribution Figure 2 can be described by the following equation [30].

$$f(V) = \frac{k}{c}\left(\frac{V}{c}\right)^{k-1} \exp\left[-\left(\frac{V}{c}\right)^{k}\right] \tag{1}$$

where k is shape factor, c is the scale factor and V represent the wind speed. The cumulative density function is calculated as follow:

$$F(V) = 1 - \exp\left[-\left(\frac{V}{c}\right)^{k}\right] \tag{2}$$

3.2 Maximum Likelihood Method

The maximum likelihood method involves estimating the parameters of the Weibull distribution (shape and scale parameters) that maximize the likelihood of observing the wind speed data. The maximum like–lihood method involves minimizing the difference bet–ween the observed wind speed data and the Weibull distribution function using numerical optimization methods [30].

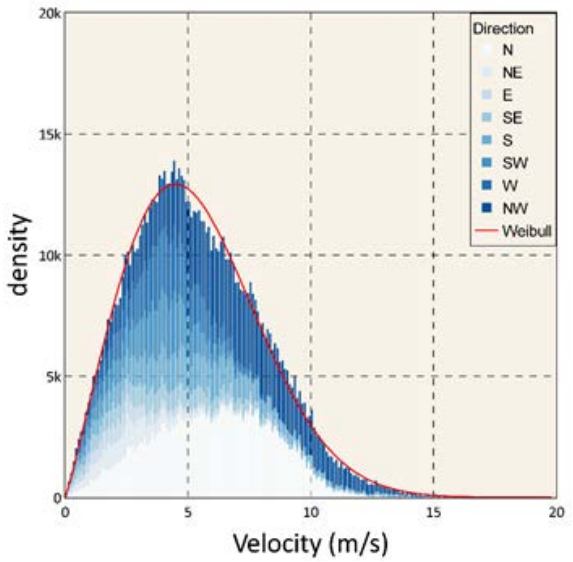

Figure 2. Weibull distributions for wind speeds

$$k = \left(\frac{\sum_{i=1}^{n} V_i^k \ln(V_i)}{\sum_{i=1}^{n} V_i^k} - \frac{\sum_{i=1}^{n} \ln(V_i)}{n}\right)^{-1} \tag{3}$$

$$c = \left(\frac{\sum_{i=1}^{n} V_i^k}{n}\right)^{\frac{1}{k}} \tag{4}$$

k and c, are function of altitudes, and therefore, for the corresponding hub heights they estimated as follows [31]:

$$k = k_0 \frac{1-0.0881\ln(z_0/10)}{1-0.0881\ln(z/10)};\ c = c_0\left(\frac{z}{z_0}\right)^{\beta};\ \beta = \frac{0.37-0.0881\ln c_0}{1-0.0881\ln(z_0/10)} \quad (5)$$

where k_0 and c_0 are the parameters at the reference elevation z_0, and z is the hub height.

3.3 Wind Energy Calculations

The mean wind velocity V_m and standard deviation σ are estimated as follows [32].

$$V_m = c\Gamma\left(1+\frac{1}{k}\right);\ \sigma = c\left(\Gamma\left(1+\frac{2}{k}\right)-\Gamma^2\left(1+\frac{1}{k}\right)\right)^{0.5} \quad (6)$$

The wind power density P_d and wind energy E are given as: (t is the time period, Γ is the Gamma function, and ρ is air density)

$$P_d = \frac{\rho c^3}{2}\frac{3}{k}\Gamma\left(\frac{3}{k}\right);\ E = P_d t \quad (7)$$

The most frequent wind speed V_{fmax} and the velocity V_{Emax}, that yields maximum output energy are calculated as follows:

$$V_{f\max} = c\left(\frac{k-1}{k}\right)^{\frac{1}{k}};\ V_{E\max} = c\left(\frac{k+2}{k}\right)^{\frac{1}{k}} \quad (8)$$

The output power density for any model turbine is estimated using (Manwell et al. 2010).

$$P_{d,output} = \begin{cases} 0 & V < V_{cut\,in} \\ P_d & V_{cut\,in} < V < V_{rated} \\ P_{d,rated} & V_{rated} < V < V_{cut\,out} \\ 0 & V_{cut\,out} < V \end{cases} \quad (9)$$

where $V_{cut\ in}$, $V_{cut\ out}$, V_{rated}, and $P_{d,rated}$ are the cut-in speed, cut-out speed, rated speed, and power density at rated speed; respectively. The capacity factor for a wind turbine is found as:

$$CF = \frac{P_{d,output}}{P_{rated}} \quad (10)$$

4. ELECTRIC VEHICLE CHARGING STATION

4.1 Characteristics of Common Electric Vehicle Charger Levels

The most common levels of electric vehicle chargers established by SAE International include Level 1, Level 2, and Level 3/DC Fast Charging. Level 1 chargers use a standard 120V outlet and are best suited for locations where vehicles are parked for extended periods overnight or during the workday. Level 2 chargers are typically located where vehicles are parked for an extended period, like at homes, apartments or workplaces, as they allow drivers to charge their EVs over the course of a few hours while doing other activities like relaxing at home or working at the office. Level 3 fast chargers are commonly placed along major roads and highways where people are traveling between locations. The faster charging capability suits drivers who need to quickly charge before continuing their journey. Level 3 chargers help minimize stops for those constantly on the go. They can also be useful for commercial fleet vehicles that cover large distances daily and need to charge rapidly to maximize uptime. Given that the current study involves designing an electric vehicle charging station for a highway location, Level 3 fast charging would be the most appropriate option since it best suits the needs of drivers.

4.2 Load Assessment

The proposed charging station would be located along various locations along the Red Sea coast to facilitate electric vehicle travelers and commercial transport between these major population centers. A renewable energy microgrid, employing hybrid wind-battery technology, is well-suited to provide zero-carbon power independent of the main electric grid, in this remote coastal area. The station would contain four 50 kW direct current (DC) fast chargers to serve the growing electric vehicle traffic demands. Auxiliary energy loads accounted for in the feasibility analysis include EV supply equipment controls, interior and exterior lighting for the facility and surrounding area, heating ventilation & air conditioning (HVAC) systems to maintain comfort year-round, an on-site 100 kW backup diesel generator, battery storage and associated power condi–tioning equipment for energy time-shifting and resili–ence during intermittent generation periods from wind. Peak energy needs will include power requirements for supplemental infrastructure like on-site labor housing units, a convenience and coffee shop and prayer room to support station workers and visitors.

The majority of fast chargers installed worldwide are currently limited to 50kW rated capacity. However, several projects have recently been announced to install fast charging points up to 350kW. Currently, there are no EVs capable of accepting a 350kW charge (Bryden et al. 2018). With this in mind, it is estimated that the power demand of each DC fast charger could reach 50 kW while in use. Lighting, HVAC and other constant facility loads are projected based on building designs accounting for the coastal climate. The backup generator and battery storage inverters are each sized to provide 100 kW of redundant power capacity during periods when the charging station must continue operating without wind assistance. Table 2 summarizes these peak load estimates for the major energy consuming components that the renewably-powered microgrid must adequately supply using locally harnessed wind energy. These load estimates are based on the following assumed requirements: a) DC fast chargers estimated at maximum 50 kW each, b) interior lighting load ~300 m^2 facility size, c) Interior and

exterior lighting includes parking area, d) HVAC sized for 650 m^2 total facility area, d) Battery storage scaled to provide 1-hour backup at total peak load, e) Labor housing for 5 residential units, f) Shop/workshop sized for minor maintenance/repairs, g) prayer room estimated at 50 m^2, h) coffee shop estimated at 100 m^2 space, including coffee brewing/storage, refrigeration, lighting, small kitchen, for simultaneous food prep and customer usage. In this case the total peak load is rounded up to 400 kW for feasibility analysis.

A detailed load assessment must involve developing an hourly/sub-hourly energy demand profile for the charging station and associated facilities over different timescales to appropriately size the renewable microgrid system. Key components should be analyzed to determine their estimated peak power loads under worst-case operating scenarios, accounting for equipment specifications, typical usage patterns, environmental conditions, and occupancy. Assumptions are usually made on facility attributes like building area and expected processes to estimate equipment counts. The current modeling establishes the maximum instantaneous power requirements and total energy needs that the integrated wind and battery resources must reliably meet on an around-the-clock basis. Particularly, the projected total peak load serves as the baseline capacity target for system design. Through load profiling, the microgrid design can be optimized to meet demand while avoiding over or under-sizing generation, ensuring technical feasibility and supporting project economic viability over the long-term.

The current feasibility analysis will determine if the identified sites can reliably meet the projected 400 kW load. Multiple wind turbine models will be evaluated to identify the best technology for each location, considering wind turbine power curves, and capacity to reliably meet the 400 kW peak load over the charging station's lifetime. If feasible, this study could demonstrate innovative renewable energy solutions for powering onshore infrastructure for electric vehicle adoption along coastal highways nationwide.

Table 2. Estimated Peak Energy Loads for Proposed Charging Station (N = number of charging ports)

Load Component	Peak Load (kW)
DC Fast Chargers (N × 50 kW)	50 N
Lighting (facility & grounds)	25
HVAC Equipment	45
Battery Energy Storage Systems	75
Housing Units (5)	15
Convenience Shop	10
Multipurpose Hall	5
Coffee Shop/Cafe	20
Bathroom Facilities	5
Total Peak Load	50 N + 200

4.3 Sizing the Wind Generation Asset Based on Predicted Energy Performance

Capacity factor is a performance metric used to evaluate the expected long-term energy output of wind power systems. It represents the ratio of actual energy produc–tion over a given period to the theoretical maximum output if the system operated at full nameplate capacity continuously. To properly size the wind turbine instal–lation cpacity to meet the facility's energy demands, a standard capacity factor analysis is performed. The capacity factor is determined based on regional wind resource data and the wind turbine power curve. It represents the long-term average power production of the turbines compared to the theoretical maximum output rating and accounts for variability in wind speeds and downtime over the course of a year that affects the total annual energy generated. In the methodology adopted, the total facility load is used to determine the average annual energy production target required from the wind turbines. This energy target is then divided by the capacity factor to calculate the necessary installed wind turbine capacity needed to be deployed to achieve the annual generation goal and reliably. By following this methodology, which relates the site loads to energy output capacities based on realistic wind resource assumptions and the wind turbine power curve, the optimal turbine configuration can be identified to cost-effectively meet the microgrid's power demands. A thorough evaluation is conducted of 36 different wind turbine models spanning from 1.5MW to 4MW capa–cities. The characteristics of each turbine type are sum–marized in Table 3. These turbines are comprehensively analyzed based on the annual capacity factor data to determine their reliability in activating concurrent EV charging port levels across the nine locations under consideration.

4.4 Energy Storage Requirement

To provide a stable output from the wind-powered system, a battery storage system (BSS) is required. This is due to the intermittent nature of wind speed. The BSS utilizes lithium-ion battery technology, offering a depth of discharge of 80% and 96% efficiency along with an impressive life of 10,000 cycles.

The inclusion of the BSS improves the stability of the system, allowing an uninterrupted power supply for EV charging while efficiently utilizing wind energy. When energy output from the wind turbine exceeds demand, the BSS can be charged and the excess energy stored. Leading Class 3 EV charging equipment like the BTCPower Matrix, XCharge Megawatt or Power Electronics ARC stations could provide this with optional battery capacities scaled to the site's average daily or weekly demand.

Table 3. Specifications for the 36 selected turbines used in site assessment

Wind Turbine Model	Hub height (m)	Cut-in Speed (m/s)	Rated Speed (m/s)	Cut-out Speed (m/s)	Rotor Dia (m)
Selected 1.5 MW Rated Power Turbines					
Dongfang FD93-1500	80	3	9.5	20	93
Goldwind GW 87 / 1500	85	3	9.9	22	87
Lagerwey L100 1.5 MW	135	2.1	10	28	100

SANY SE10015	80	3	10	22	102
MingYang MY1.5/89	100	3	10	25	89
Envision EN 87-1.5	70	3	10	25	87
Windey WD93-1500	80	3	10.1	20	93
GE 1.5xle	80	3.5	11.5	20	82.5
Nordex N82	80	3.5	12	25	82
Selected 2 MW Rated Power Turbines					
SANY SE12520	90	2.5	8.5	22	125
Windey WD121-2000	140	2.5	8.6	20	121
Dongfang G2000-116	90	3	9	20	116
MingYang MY2.0/118	90	3	9.5	25	118
AMSC wt2000fc TC	100	3	11	20	113
Vestas V100-2.0	120	3	12	22	100
Hitachi, Ltd. HTW2.0-86	78	4	12	24	86
Soyut Wind 2000	50	4	12	25	88
Enercon E-82 E2 2.000	138	2	12.5	34	82
Selected 3 MW Rated Power Turbines					
Windey WD140-3000	140	2.5	9.1	25	140
MingYang MySE3.0-135	140	3	9.3	20	135
SANY SE12730	138	3	9.5	25	127
Goldwind GW 140 /	120	2.5	10.5	20	140
Dongfang G3000-119	90	3	10.5	20	119
Nordex N131/3000	134	3	10.5	20	131
Envision EN 120-3.0	90	3	11	25	120
Aerodyn SCD 3.0/115 basic	85	3	11.5	20	115
Senvion 3.0M122	122	3	11.5	22	139
Selected 4 MW Rated Power Turbines					
Suzlon S 146	160	3	9	20	146
MingYang MySE4.0-156	140	2.5	9.7	25	156
Envision EN 136-4.0	80	3	10	25	136
Goldwind GW 136 /	110	2.5	11	25	136
Dongfang D4000-148	90	2.5	11.5	20	148
Vestas V117-4.2	114	3	12	27	117
Enercon E-126 EP3	135	2	12.1	30	127
Siemens SWT-4.0-120	90	4	13.5	32	120
GE General Electric GE 4.1-113	85	3.5	14	25	113

5. RESULTS AND DISCUSSION

This section provides an in-depth evaluation of the wind resource potential and viability for powering electric vehicle charging stations at nine coastal locations along the Red Sea in Saudi Arabia. Analyses were conducted on wind speed and direction data obtained from mete–orological records spanning 2014 to 2023.

The findings on the variations of average annual wind speeds observed across the different study areas are presented.

Examination of the predominant wind directions characterizing each site is also discussed. Seasonal fluctuations in wind speeds are then addressed. A Weibull distribution analysis is used to statistically characterize the regional wind patterns. The section also covers turbine performance assessments tailored to the wind conditions at each location. Finally, the EV charging capacity supported by wind turbines based on projected demands is evaluated.

5.1 Variations of Average Annual Wind Speeds Across Study Sites

The analysis of average annual wind speed results from 2014-2023 revealed notable differences among the selected locations along the west coast of Saudi Arabia [33]. Specifically, three locations on the Southwest Coast, namely Al Laith and Jazan, exhibited significantly lower average wind speeds compared to other locations. In fact, the wind speeds in these areas were approximately 30% lower than that at the remaining locations.

The relatively low wind speeds in the Southwest Coast can be attributed to the distinct topographical and climatic features that characterize this particular region of the Saudi Arabia along the Red Sea coast. A prominent topographic feature is the presence of the Asir Mountain range, which spans across the Southwest coast and acts as a barrier to northeasterly winds. Con–sidering the wind potential for power generation, the lower prevailing wind speeds in the Southwest coast areas may not provide sufficient kinetic energy to efficiently generate electricity using wind turbines. As a result, these regions may not be the most suitable for wind energy projects due to their suboptimal wind resources.

Figure 3. The yearly average wind speed (m/s) for the nine selected sites at 50 m

5.2 Predominant Wind Direction at the Selected Sites

The prevailing wind direction along the west coast (Figure 4), is influenced by global atmospheric circu–lation patterns, the regional topography, and proximity to large bodies of water. Analysis of the prevailing wind directions reveals a clear distinction between the environments in the Northwest and Midwest coastal zones versus the Southwest coast. At northerly locations, analysis reveals the dominant prevailing winds originate from northwesterly flows with greater persistence than other directions. In contrast, analysis of three southwesterly sites—Al Laith, Al Gunfuthah and Jazan— demonstrates prevailing winds predominantly from the southwest direction. This difference in prevailing winds between the upper coastal zones and southerly locales can likely be attributed to interactions between large-scale atmospheric patterns and the region's shifting coastal topographies.

5.3 Wind Speed Seasonal Variation

Understanding of the seasonal change of wind speed is important to match the load of the area based on the wind power availability. In Saudi Arabia, usually the load is high in summae time due to excessive usage of air-conditioning systems. Figure 5 shows the seasonal variation in wind speed for the selected locations. The Northwest and Southwest coasts show two different wind speed patterns and seasonal changes. The northwest coast had three of the highest four potential areas and showed the highest average monthly wind speeds in January-February and April-September. The lowest monthly average wind speeds are seen in March and October-December.

The seasonal variations in wind speeds can be partly attributed to changes in atmospheric pressure systems, the temperatures, and wind circulation patterns throug–hout the year. In winter months, the region typically experiences stronger north-easterly winds as lower pressure systems track over the Mediterranean Sea and northern Saudi Arabia. During spring and summer, wind speeds remain high along the northwest coast due to the formation of a thermal low over the Middle East, strengthening pressure gradients and wind flows. On the other hand, the Southwest coast had average wind speeds approximately 30% less and showed the lowest monthly wind speeds in January, February, and August. This is likely due to the topographic influence of the Asir Mountains disrupting and weakening winter wind flows, along with weaker pressure systems tracking over the Gulf of Aden during summer. The seasonal differences can also be attributed to the different atmospheric conditions and topography between coasts. For example, the Northwest Coast is located closer to the Mediterranean Sea and experiences a predominantly north-easterly wind, while the Southwest is closer to the Gulf of Aden and Indian Ocean with a predominantly easterly and south-easterly wind regimes.

5.4 Characterizing Regional Wind Patterns using Weibull Analysis

Figure 6 illustrates the wind speed probability distributions for the nine sites based on 10 years of data alongside fitted Weibull curves. For each location, a histogram shows the observed frequeny of wind speeds, and a superimposed curve displays the Weibull distribution fitted to the data. Significantly, the Weibull fit closely matches the probability patterns at all locations. This strong alignment indicates the model effectively characterizes various wind regimes observed across the west coast. The Weibull distribution captures not only the overall shape but also subtle variations between sites. The close fit provides confidence in using Weibull parameters derived from the measured data. Metrics like the shape and scale parameters provide meaningful insights into energy potentials. The Weibull distribution is highly useful for energy modeling like production forecasting under varied scenarios.

Table 4 provides a technical analysis of the wind resource potential across nine coastal cities. By characterizing the Weibull distribution parameters, sig–nificant insights are gained regarding variations in wind conditions and energy conversion. The shape (k) and scale (c) parameters effectively model the frequency of wind speeds, directly correlating to predicted power outputs. Average wind speed (V_m), peak probability speeds (V_{fmax}), and wind speed corresponding to maxi–mum energy capture (V_{Emax}) are useful indicators for preliminary energy estimation. Ultimately, the derived power density (P_d) and annual energy generation values (E_d) benchmark the sites on a common scale.

The analysis revealed substantial divergences bet–ween the selected regions. The three cities in the south–west exhibit signs of limited wind power viability, with median wind speeds below 5 m/s correlating to power densities of 105 W/m^{2}or below it. In contrast, the five locations (Neom, Duba, Umluj, Yanbu and Jeddah) along the northwest and central coastal regions demon–strate more favorable wind resources for productive harvesting. Surpassing average speeds of 5.3 m/s, distri–butions show higher probabilities of winds exceeding typical turbine cut-in thresholds. Accordingly, wind power densities exceed 150 W/m^2 and annual output values reflect stronger energy conversion potential.

These variances characterize the climatic determinants of viable wind power deployment across diverse coastal topographies. The analysis revealed variation in wind potential across sites, most locations—except Yanbu and Neom—demonstrated limited prospects for wind energy projects. However, when benchmarked against the National Renewable Energy Laboratory's (NREL) wind resource classification system, only Yanbu and Neom fell within the marginal wind power class, Table 5. This indicates that these areas may have some potential for wind energy development.

However, it is important to note that power density alone does not provide a complete assessment of a site's wind resource potential. Additional factors like wind speed variability, turbulence, and atmospheric stability may also influence the feasibility of wind power projects. Key wind characteristics, beyond power density, are considered to better understand each location's suitability for wind energy generation.

Table 4. Annual wind characteristics for all sites

Location	Latitude (°N)	k	C (m/s)	V_m (m/s)	V_{fmax} (m/s)	V_{Emax} (m/s)	P_d (W/m^2)	E (kW/m^2.y)
Neom	28.12	2.09	6.45	5.71	4.73	8.88	208.31	1824.82
Duba	27.15	2.09	6.02	5.33	4.41	8.29	169.69	1486.48
Umluj	25.52	2.24	6.01	5.33	4.62	7.99	159.05	1393.29
Yanbu	24.40	2.63	6.89	6.12	5.75	8.54	213.89	1873.70
Rabigh	23.35	1.96	4.96	4.40	3.45	7.10	101.55	889.59
Jeddah	20.98	2.13	6.06	5.37	4.49	8.28	170.56	1494.13
Al Laith	20.05	1.85	4.27	3.80	2.81	6.34	69.26	606.75
Al Gunfuthah	18.56	1.95	4.96	4.40	3.43	7.14	102.68	899.51
Jazan	17.50	1.76	4.03	3.59	2.51	6.20	62.09	543.90

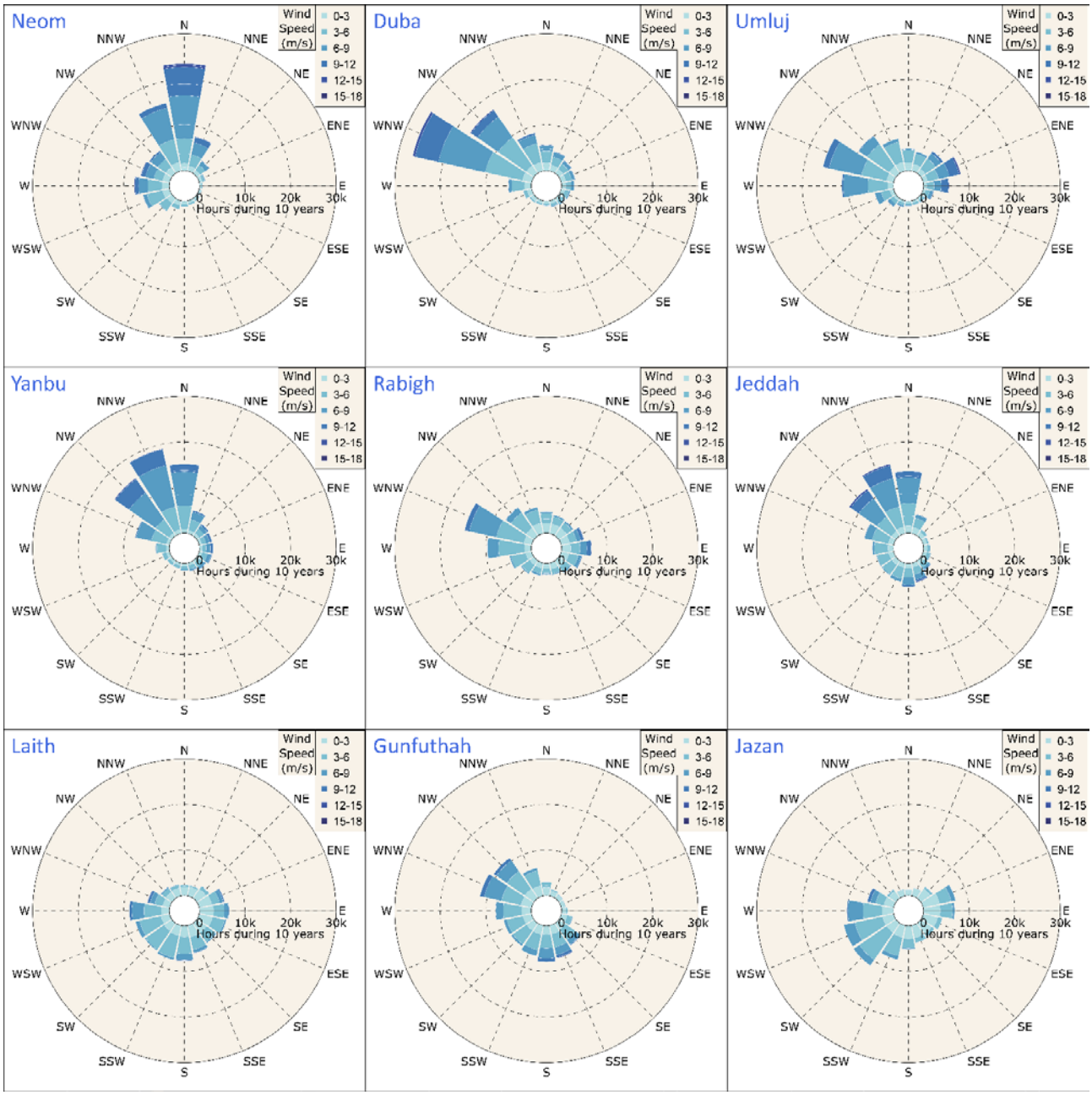

Figure 4. Wind direction and speed for the selected locations

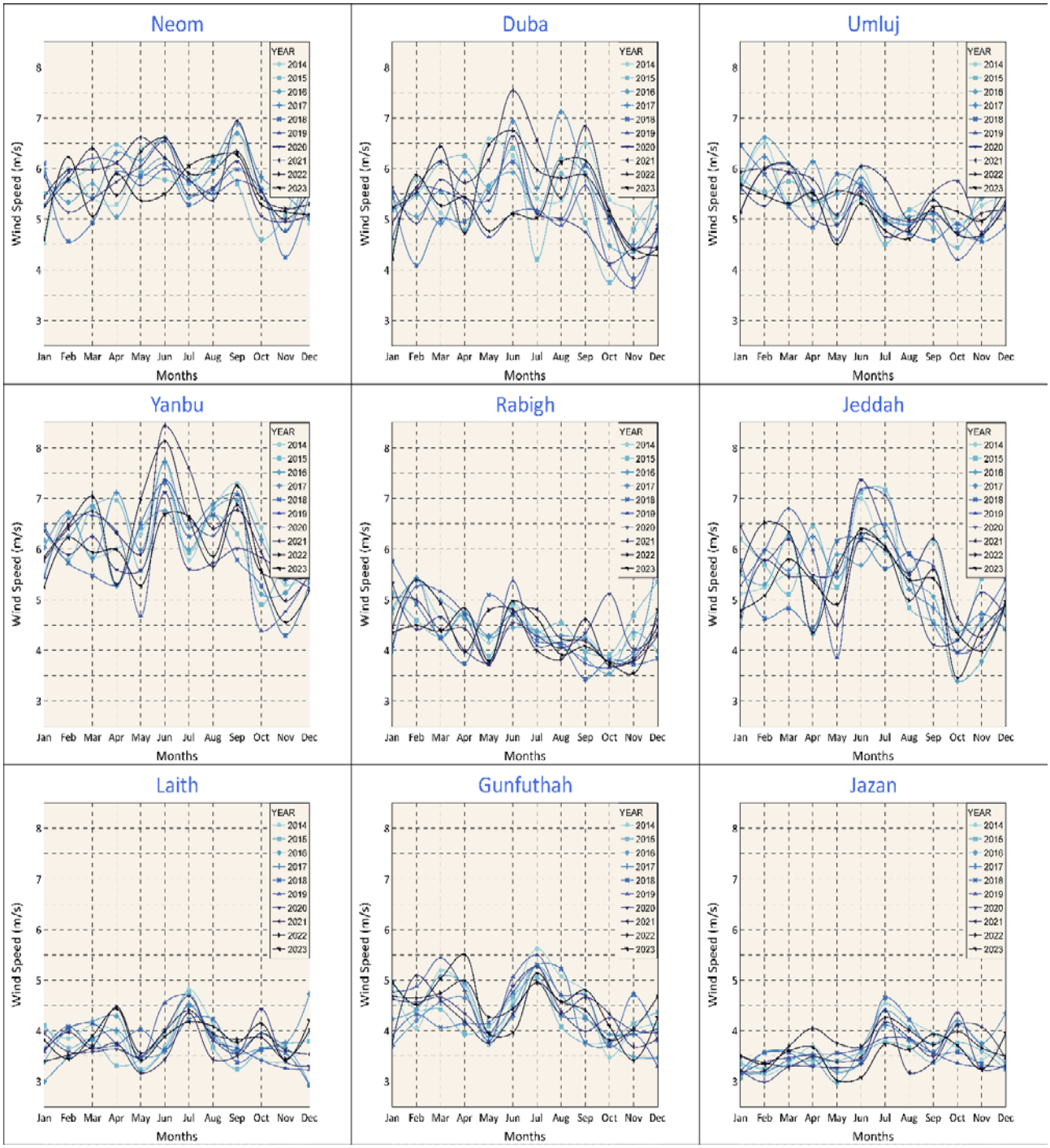

Figure 5. Seasonal (monthly average) variation in wind speed for the selected locations

Table 5. Calculated power density and NREL wind class

Location	Power density (W/m^2)	NREL Wind class
Neom	208.31	Marginal
Duba	169.69	Poor
Umluj	159.05	Poor
Yanbu	213.89	Marginal
Rabigh	101.55	Poor
Jeddah	170.56	Poor
Al Laith	69.26	Poor
Al Gunfuthah	102.68	Poor
Jazan	62.09	Poor

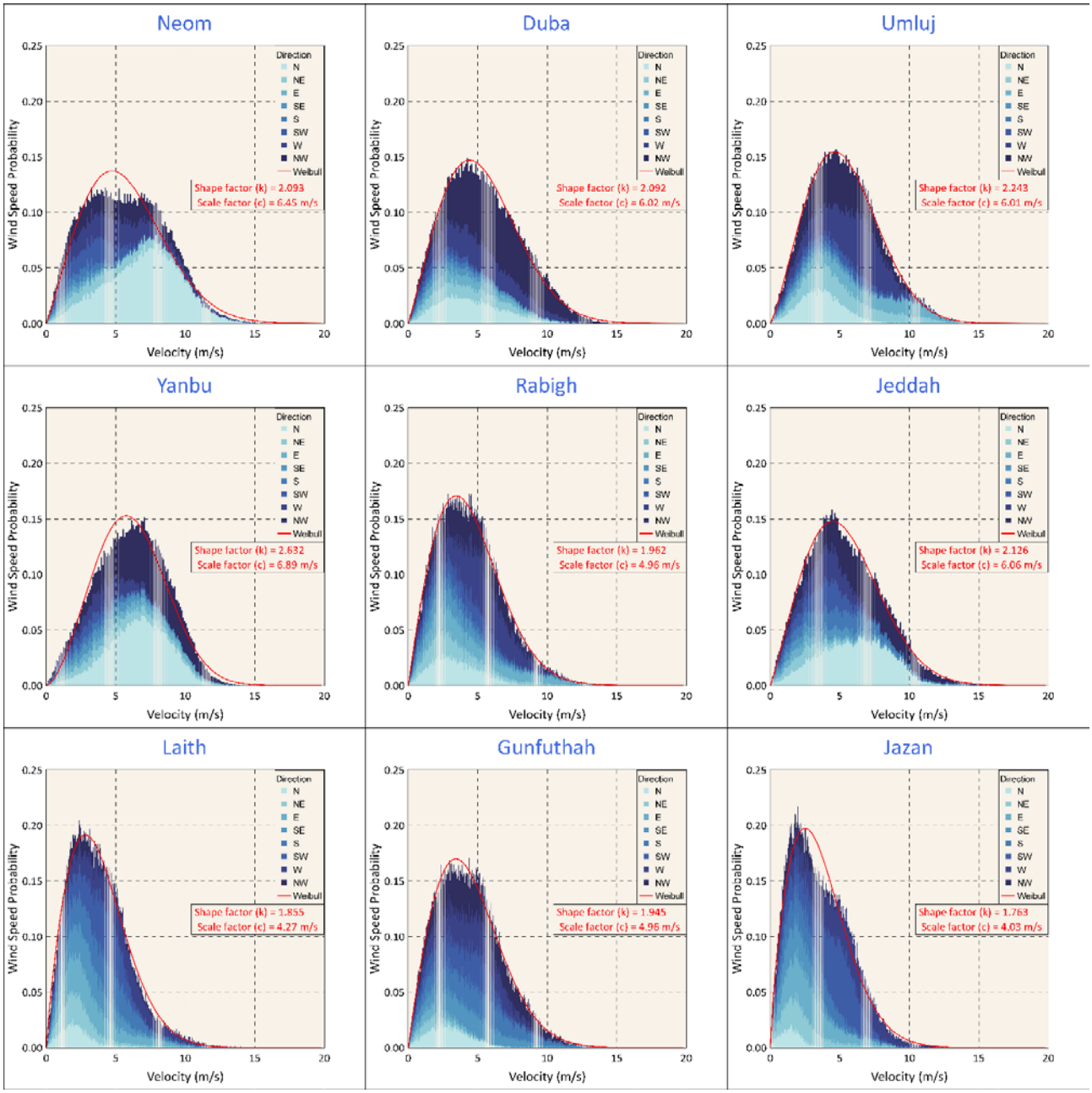

Figure 6. Measured probability density distribution and fitted Weibull distribution for all selected sites

5.5 Wind Turbine Performance Assessment at the Selected Sites

This section examines capacity factor data for wind turbines ranging in size from 1.5 MW to 4.0 MW across all the sites. The data is evaluated to support planning of locations for wind-powered EV charging stations. Optimal siting of charging infrastructure requires understanding how turbine productivity may vary both with technology and wind resources. A total of 36 turbine models are assessed for each of 1.5 MW, 2.0 MW, 3.0 MW, and 4.0 MW rated capacities. Some details about these selected turbine models are summarized in Table 3 above. When selecting a system for the proposed EV charging stations, the seasonal and annual wind resources variability is important. Box plots are utilized to identify how annual capacity factors differ for each turbine-site combination based on 10-year simulations. Comparing detailed performance trends to determine which combinations are best suited to reliably power EV charging stations and supporting continued expansion of sustainable transportation.

Figure 7 shows the distribution of annual capacity factors for each 1.5 MW turbine model across the 9 simulated sites.. Each box shows the interquartile range (IQR) of the data, which is the difference between the 25th and 75th percentiles, with a line at the median. The "whiskers" extend to the highest and lowest values, excluding outliers which are plotted individually. Each of the 9 graphs represents one site, for the selected 1.5 MW capacity turbines. On the x-axis, the turbines are spaced equally from left to right, though their actual rated wind speeds increased from 9.5 m/s to 12 m/s (Table 3). The box plots reveal some interesting trends in the capacity factors of the selected

turbines under varying site conditions. In general, an inverse relationship can be seen between rated wind speed and achieved capacity factor, as expected from turbine performance curves. Turbines with lower rated speeds of 9.5-10 m/s tend to perform better on average across most sites. Some sites, such as Rabigh, Laith and Jazan, exhibit more consistent capacity factors over the years with less spread in the IQR boxes. Meanwhile, sites like Duba, Yanbu and Jeddah show higher variability between turbine performances, indicating less consistent wind patterns. Having no outlier points in the box plots indicate no individual yearly extremes. Some of the highest median capacity factors were observed for the Dongfang FD93-1500 turbine, ranging from 0.316 at Neom to 0.108 at Jazan.

The box plot in Figure 8 shows the variation of capacity factors with increasing turbine size from 1.5 MW to 2.0 MW. The SANY SE12520 achieved the highest median capacity factors between 0.374 at Neom and 0.147 at Jazan, comparable to top performing 1.5 MW turbines. Sites like Rabigh, Laith and Jazan continued exhibiting relatively small capacity factors for most 2.0 MW sized wind turbines. Locations with greater variability for 2.0 MW turbines included Duba, Yanbu and Jeddah, where the capacity factors Enercon dropped below 0.08. Comparatively, the average capacity factors reduced more substantially for some turbines such as Soyut and Enercon for 2.0 MW sized wind turbines.

Figure 9 depict capacity factor variability for 3.0 MW rated capacity wind turbines. The Windey WD140-3000 achieved the highest median CFs from 0.315 at Neom to 0.121 at Jazan. Similarly, Figure 10 shows capacity factor for each selected turbine in the 4.0 MW range for the 9 sites under consideration. The Suzlon S 146 achieved the highest median CFs ranging from 0.312at Neom to 0.122 at Jazan.

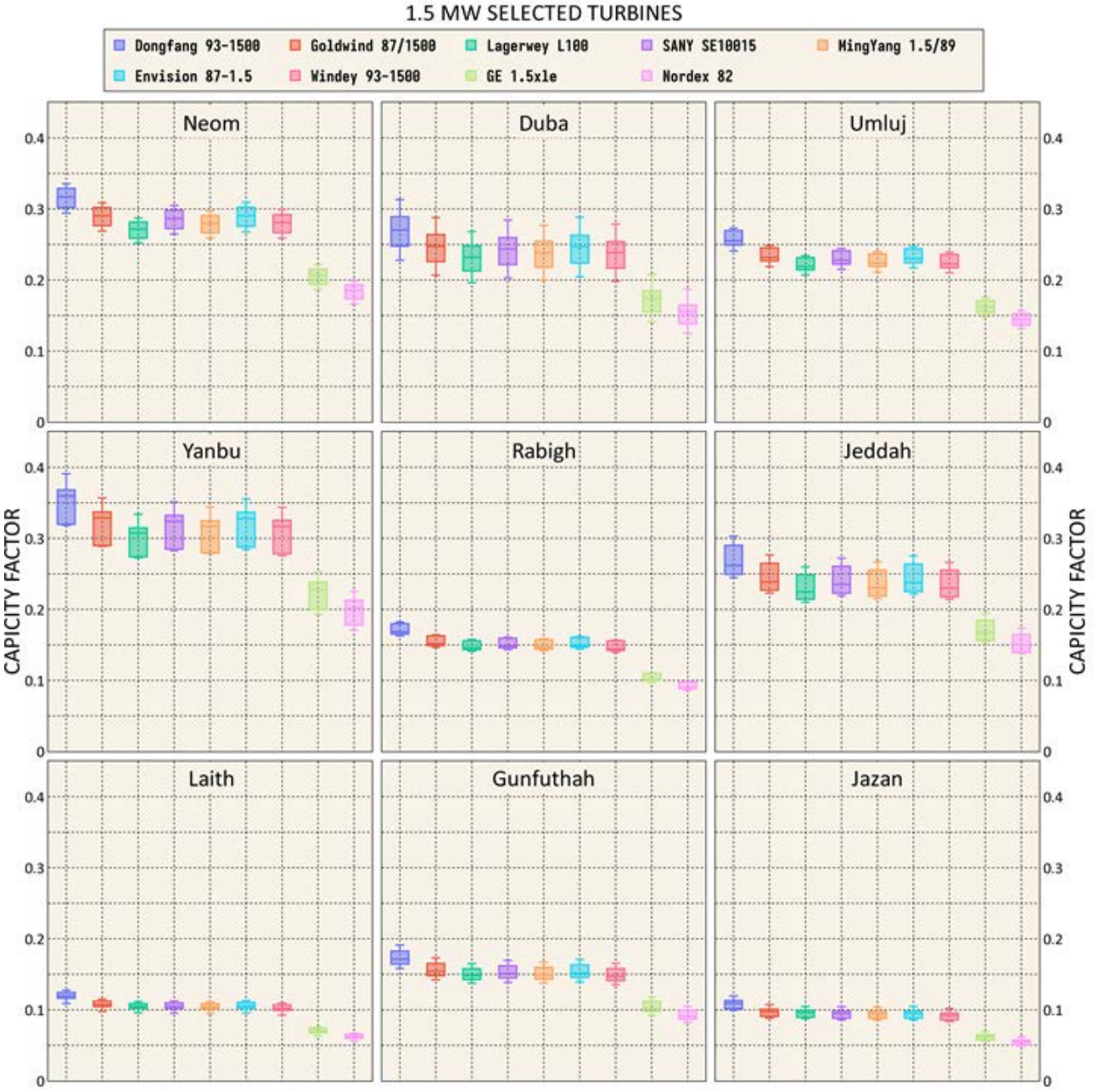

Figure 7. Capacity factor for 9 selected 1.5 MW turbines for all selected sites

The capacity factor distributions provide valuable insights for strategically deploying wind-powered EV charging infrastructure. Both component sizing and local wind conditions must be carefully considered during techno–logy selection for each charging location. Ongoing rese–arch can further optimize siting and turbine scaling to maximize energy yields available for powering electric vehicle adoption and transitioning the transportation sec–tor towards a greener future. When selecting a wind power system for the proposed charging station project, accounting for differences in annual variability is impor–tant. However, economic assessments, which are left for future study, are required to determine a specific location's optimal wind turbine model. The economic assessment should consider factors such as the cost of the wind tur–bine, installation, maintenance, and electricity to deter–mine the levelized cost of energy, simple payback period, and overall financial viability of wind energy projects.

5.6 Evaluation of Electric Vehicle Charging Capacity Supported by Wind Turbines

In addition to evaluating turbine-site capacity factor combinations, the number of concurrently active electric vehicle charging ports is also modeled to provide further insight into sustainable transportation infrastructure planning. As EV adoption grows, deter–mining optimal wind power installations to reliably meet charging demand is important. The equation (11) is used to calculate concurrently active EV ports considered both wind turbine capacity factor perfor–mance as well as an estimated auxiliary power load for supporting systems at each charging station location.

$$N = \frac{CF \times P_{rated} - P_{auxiliary}}{P_{per\ EV\ charger}} \tag{11}$$

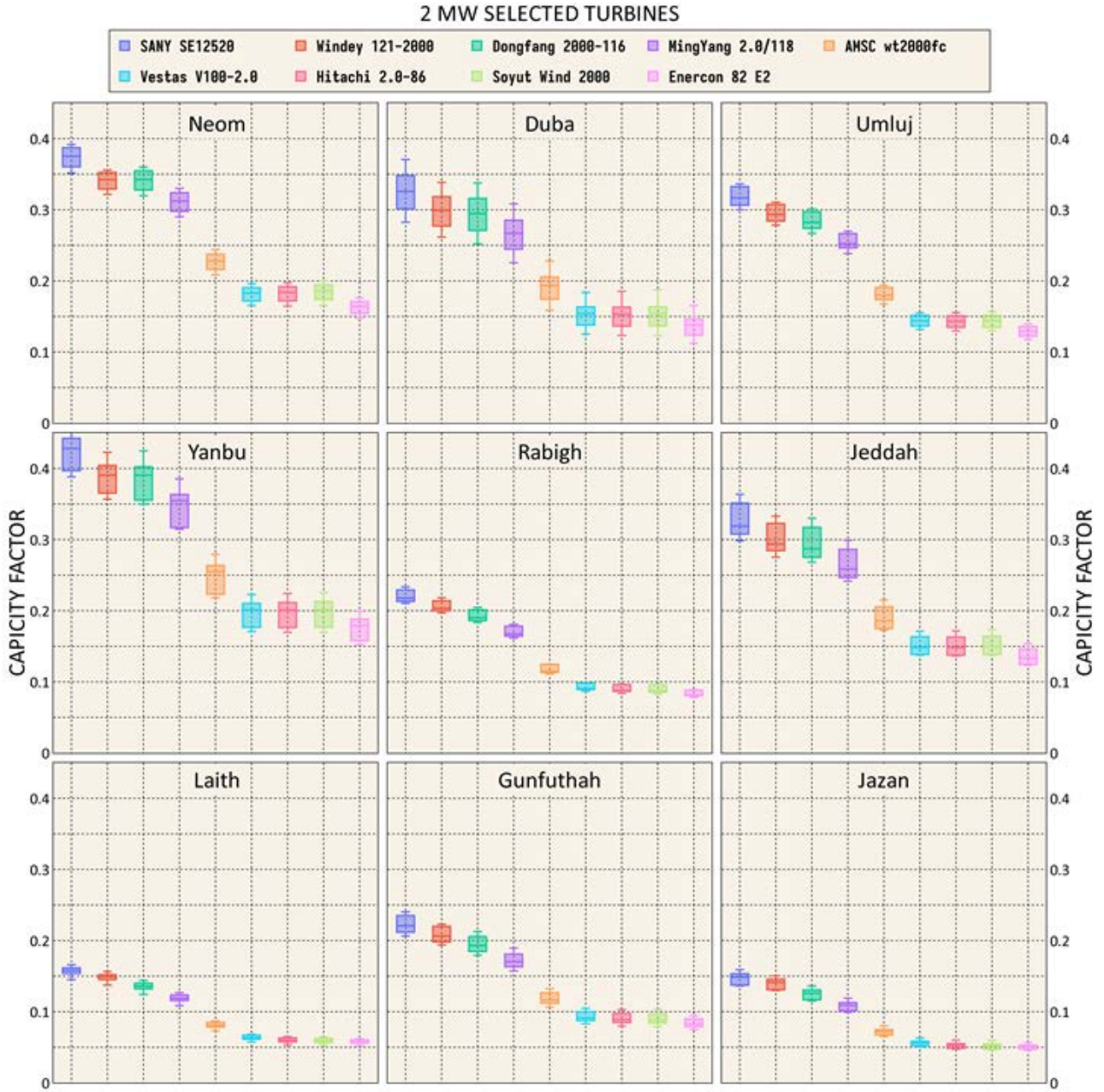

Figure 8. Capacity factor for 9 selected 2 MW turbines for all selected sites

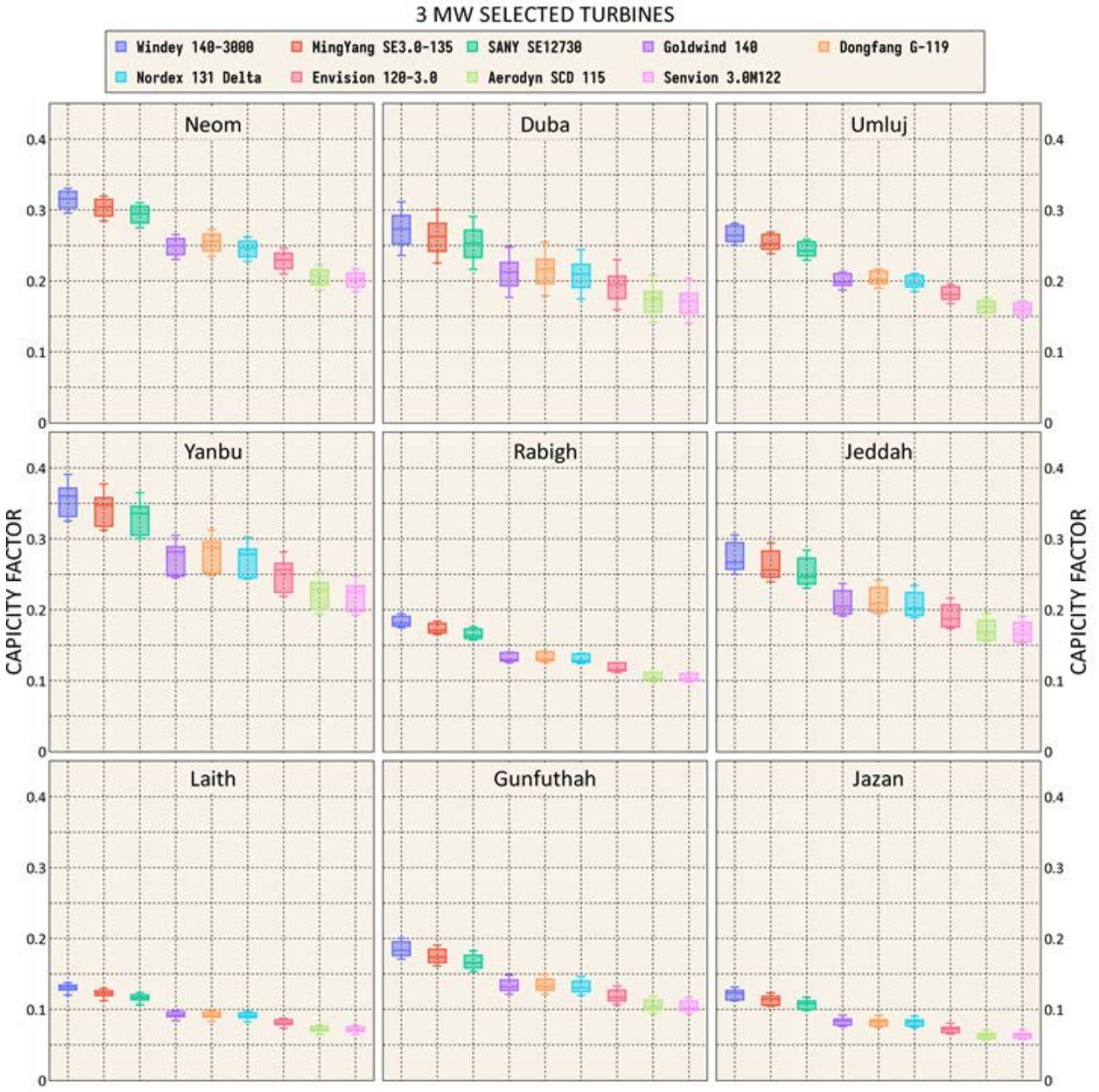

Figure 9. Capacity factor for 9 selected 3 MW turbines for all selected sites

By multiplying the rated wind turbine power output by the annual capacity factor, an estimate of available wind energy was obtained for each turbine-site. This value was then reduced by the auxiliary power needs to attain the net power available for EV charging. When auxiliary load exceeded wind generation in certain low-wind conditions, negative port values resulted, indicating insufficient renewable output to activate chargers. However, pairings with positive and consistently higher port activation levels across multiple years would be preferable. It is also important to note that the numbers of concurrently active EV charging ports shown represent annual averages, which include fractional values. This means the numbers should not be interpreted as the exact count of ports active at all times throughout the year. For example, a value of 4.5 ports for a given turbine-location combination would indicate that on average, 4 charging ports will be operational year-round to provide full-time charging availability. However, the 0.5 portion of that value suggests one additional port can be active for approximately 6 months of the year, while being inactive for rest of the months.

The box plots in 33. allow comparison of the number of concurrently active EV charging ports sup–ported by each 1.5 MW turbine-location combination based on the calculated value from annual capacity factors. In Neom, Dongfang and SANY turbines exhi–bited the highest median port activation ranging from 4.5 to 5 ports, with interquartile variability under 1 port. GE and Nordex pairs saw lower values. In Duba, Dongfang maintained the top performance with 4 active ports while GE and Nordex turbines again struggled. Goldwind and Lagerwey showed reduced port activa–tion at Neom. In Umluj, port counts declined further across most turbines, with Dongfang retaining the lead with 3.7 ports. Low-wind conditions hindered the per–formance of GE and Nordex turbines. In Yanbu, higher

resource potential boosted the performance of all the turbines, with Dongfang leading the way with above 6 active ports. Even GE and Nordex offered limited charging under 2 ports on average. Locations like Ra–bigh, Jeddah, Laith and Gunfuthah encountered serious difficulties activating EV ports for many turbines while using 1.5 MW capacity turbines due to con–sistent negative values, highlighting poor wind regimes. Over-all, Dongfang revealed a robust capability to reliably power transportation electrification across locations.

The results for 2.0 MW turbines are presented in Figure 12. For 2.0 MW turbines at Neom, SANY and Windey models exhibited the highest median port activation of more than 9 ports, with narrow interquartile ranges depicting consistent performance. Dongfang and MingYang also surpassed 7.5 ports activation on average. In Duba, Umluj and Jeddah, port counts decreased slightly but the top performers remained SANY, Windey and Dongfang with 7 ports and more. AMSC dropped to around 3.5 ports while Vestas and Hitachi fell below 2 ports. Performance continued declining at the weaker wind sites including Rabigh and Gunfuthah, however, SANY and Windey maintained leadership with over 4 ports. AMSC and Enercon struggled with fractional or negative median values. Yanbu, because of high wind potential, showed higher port activation for all the turbines. SANY peaked with more than 12 ports with Windey and Dongfang with 11 ports. Even AMSC exceeded 5 ports, a boost compared to other locations. Laith and Jazan observed extensive fractional and negative port counts while SANY and MingYang turbine were able to activate only 2 ports each.

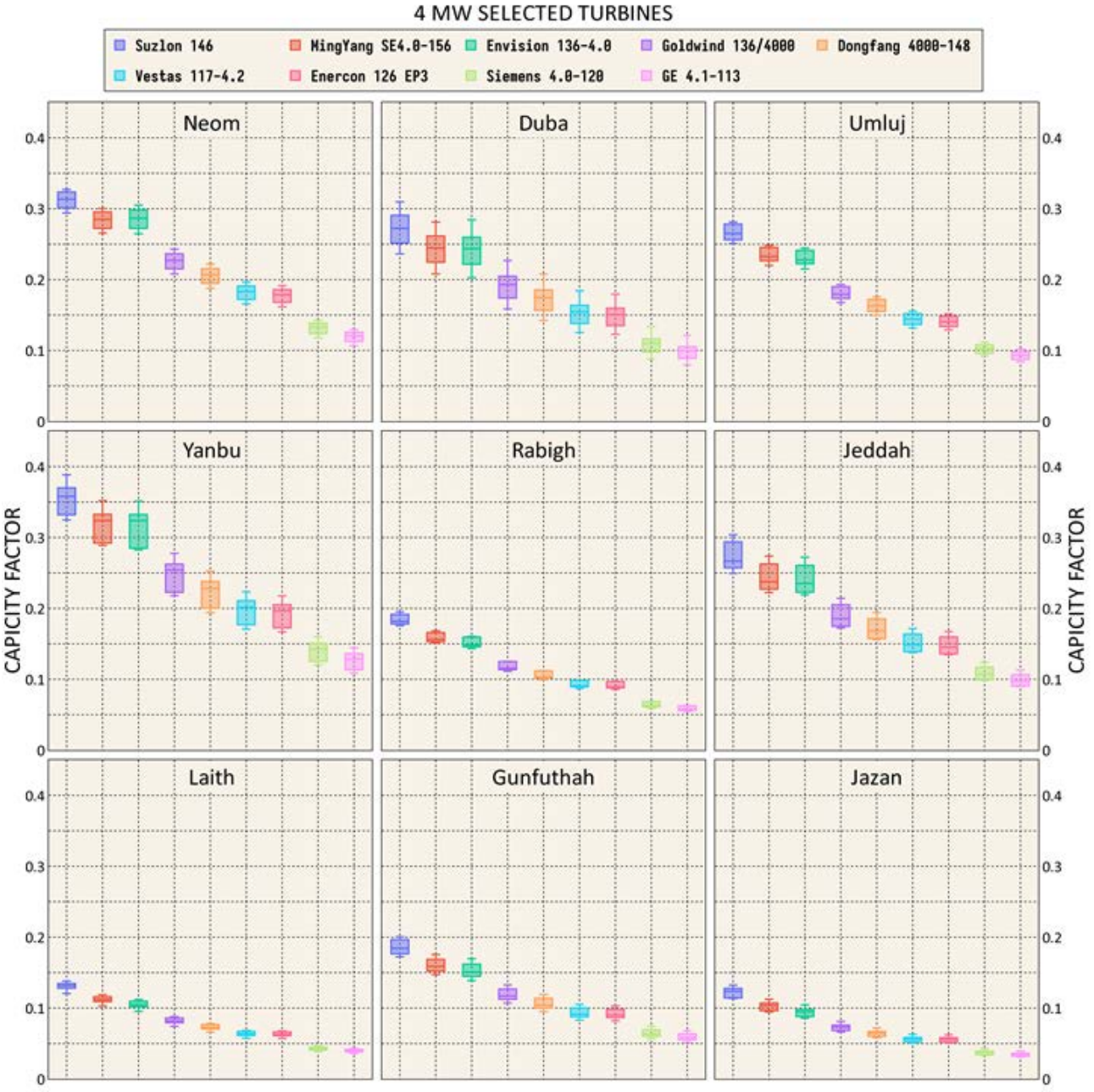

Figure 10. Capacity factor for 9 selected 4 MW turbines for all selected sites

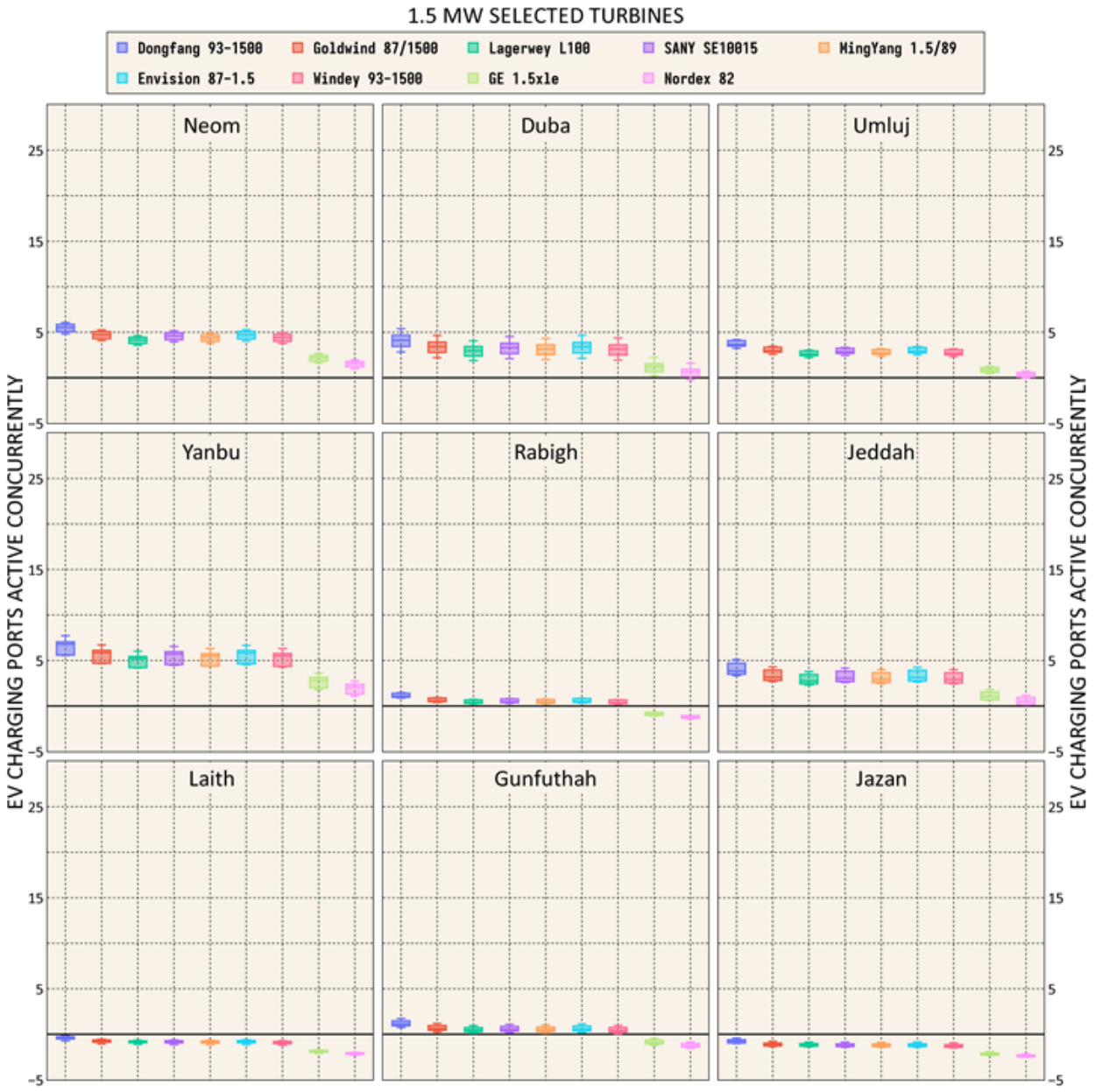

Figure 11. EV charging ports active concurrently using 9 selected 1.5 MW turbines for all selected sites. (negative value implies insufficient wind turbine power to run auxiliary systems at EV charging stations)

The results for 3.0 MW turbines, shown in Figure 13, indicate that at Neom, Windey and MingYang models demonstrated the highest median port activations exceeding 14 ports. SANY also exceeded 13 ports. Consistent interquartile ranges indicated reliable charging support at this site. In Duba, port counts remained high for top performers but declined slightly, with Windey over 12 ports. Goldwind dropped to around 9 ports while Aerodyn reamined at around 6 ports. Umluj and Jeddah showed similar trends like Duba. Yanbu's stronger winds amplified the performance of all turbines, with Windey having more than 17 active ports. Lower-wind tolerant Goldwind turbine resulted in the activation of 12.5 ports while Aerodyn was able to active 9 ports. Rabigh and Gunfuthah showed similar trends with limited port activation. Only Windey, MingYang and SANY were able to activate 6 ports on average. Laith and Jazan, as before, were weaker sites from wind resources point of view thus eliminating charging potential.

For the largest 4.0 MW sized turbines, the results are shown in Figure 14. In this case, Suzlon demonstrated premier port activation potential at all locations. At Neom, Suzlon exceeded 22 ports while MingYang and Envision surpassed 18 ports activation. In Duba, counts remained impressively high with Suzlon maintaining nearly 19 ports while MingYang and Envision sustained over 15 ports on average. Umluj and Jeddah showed similar trend to Duba as before. For Yanbu, with high wind potential, Suzlon peaked above 25 ports with MingYang and Envision over 21 ports. Even Vestas was able to activate above 12 ports. At Rabigh and Gunfuthah - Suzlon, MingYang and Envision activated 11 ports on average. Overall, Suzlon exemplified resilience powering transportation across diverse meteorological conditions.

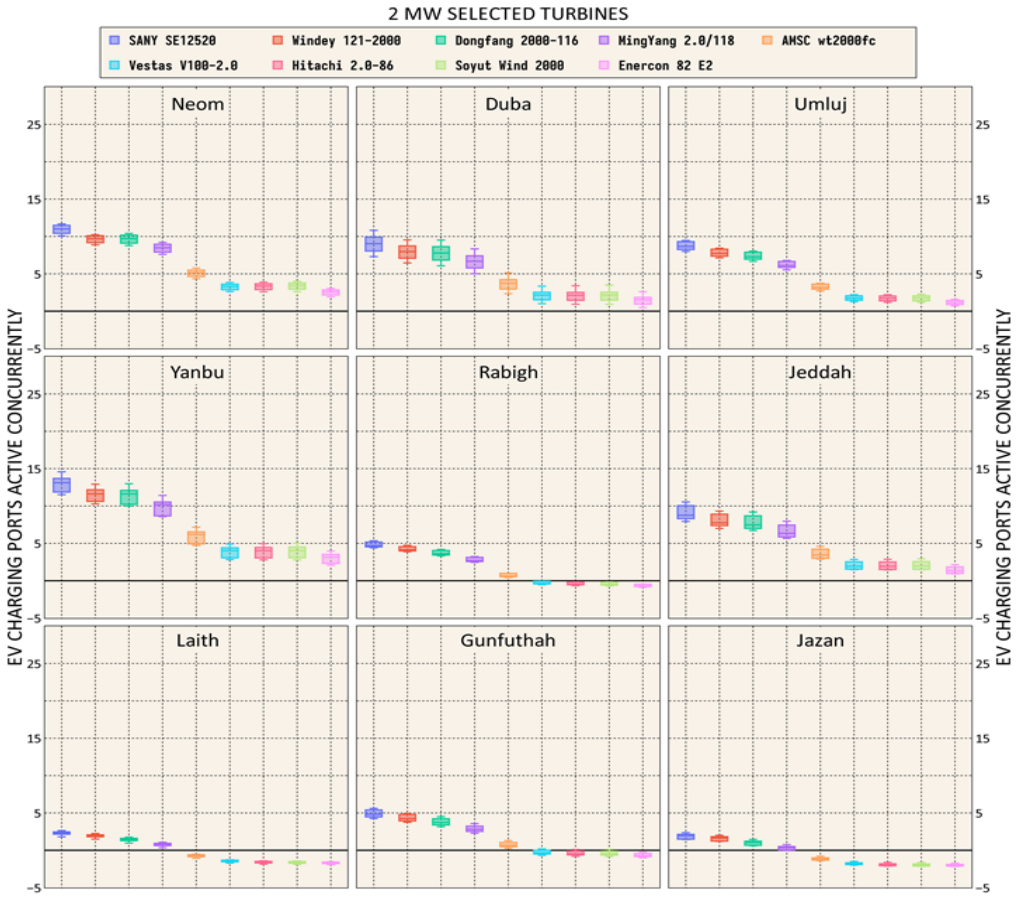

Figure 12. EV charging ports active concurrently using 9 selected 2 MW turbines for all selected sites. (negative value implies insufficient wind turbine power to run auxiliary systems at EV charging stations)

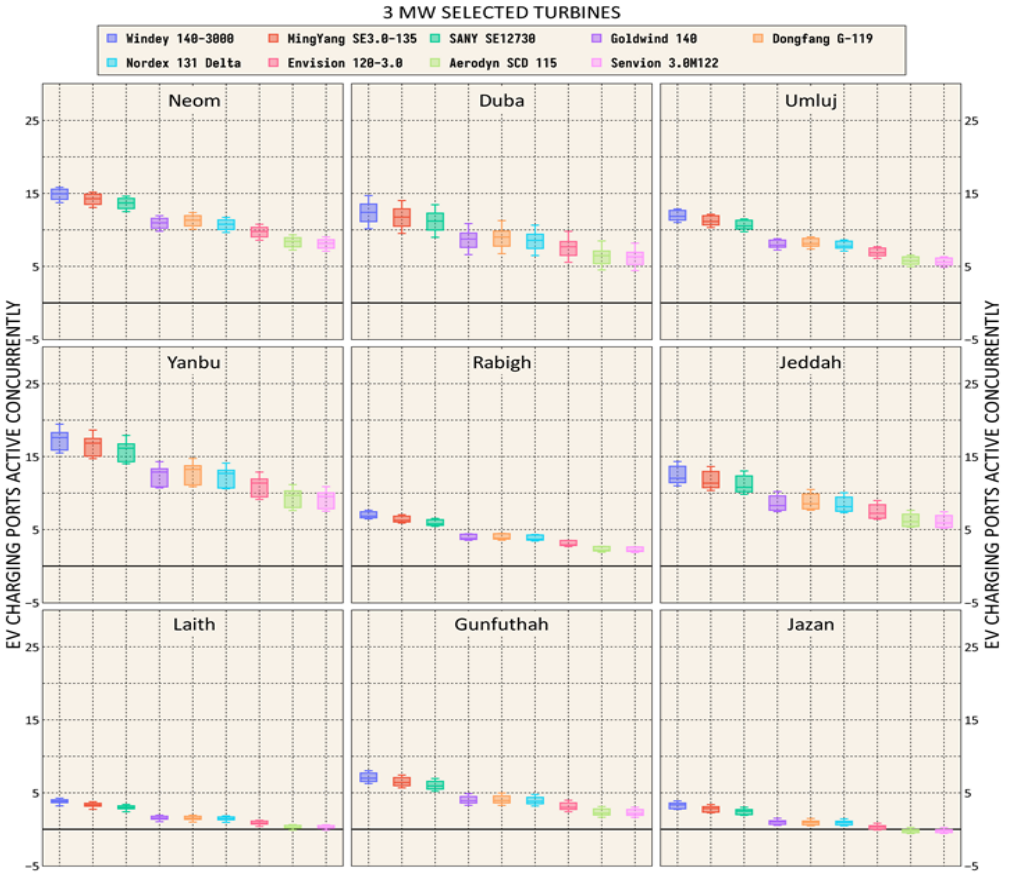

Figure 13. EV charging ports active concurrently using 9 selected 3 MW turbines for all selected sites. (negative value implies insufficient wind turbine power to run auxiliary systems at EV charging stations)

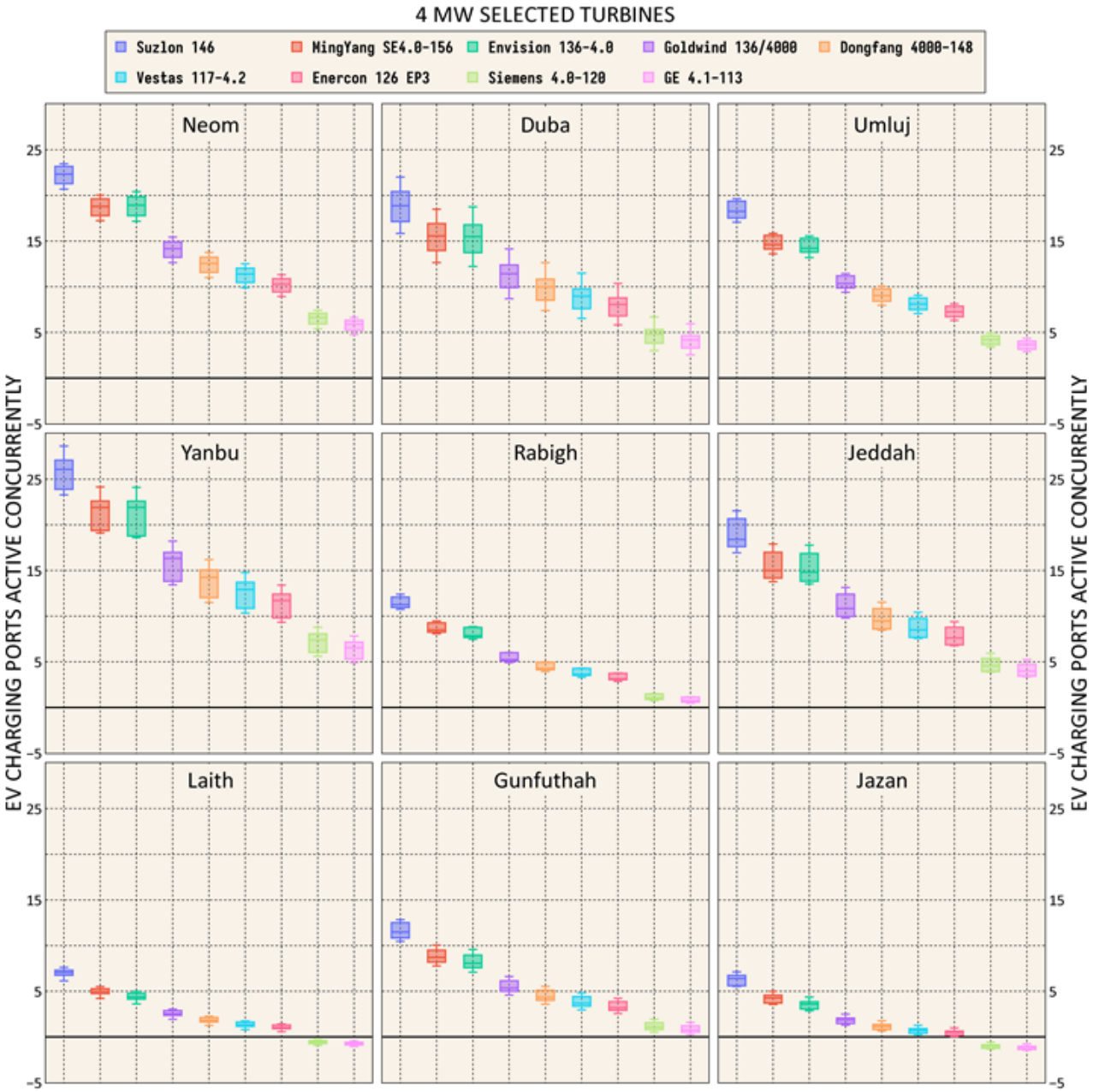

Figure 14. EV charging ports active concurrently using 9 selected 4 MW turbines for all selected sites. (negative value implies insufficient wind turbine power to run auxiliary systems at EV charging stations)

These box plots effectively benchmark turbine-site pairings, establishing frontrunners capable of consistently supporting sustainable mobility through wind-powered EV charging infrastructure under varying climate regimes. In summary, when considering the 1.5 MW rated power turbine data, Dongfang emerged as the most reliable option for supporting EV charging across all the locations due its consistently high median port activations. For 2.0 MW models, SANY and Windey demonstrated prominent stability in port activation at diverse sites. Examining the 3.0 MW rated power wind turbines, Windey, MingYang and SANY emerged as pacesetters with remarkably consistent double-digit median ports activation depending on local resource strength. Finally, among 4.0 MW sized turbines Suzlon stood to be maintaining high charging infrastructure support potentials even at locations with marginal resources. In general, progressively larger turbine models increased the number of sites viable for wind-powered EV charging. However, optimal matching to a location's wind regime remained imperative. Sites with weaker wind conditions necessitated preferential pairings showcasing endurance to low generation. This comparative evaluation effectively benchmarks different turbine-location combinations and establishes selected turbines capable of reliably meeting transportation electrification demands through wind energy. With careful multi-factor planning, the findings can help maximize deployment of wind power in support of wider sustainable mobility goals. Additional statistical analyses may further distinguish performance characteristics.

6. CONCLUSIONS

This study comprehensively evaluated the onshore wind power potential along the Red Sea coast of Saudi Arabia

to provide preliminary strategic planning for maximizing wind energy-supported transportation electrification. Nine coastal locations were selected based on 10-year hourly mean wind speed data analyzed interms of monthly/annual average speeds, wind power density classification, and Weibull modeling. The northwest locations demonstrated higher wind potential overall. However, even moderately lower wind speed sites may still be suitable with optimized technology choices. This was reinforced by wind turbine models evaluations showing that certain machines among from 1.5-4.0 MW rated capacities were capable of reliably supporting electrified transportation across various locations. Capacity factor analyses of 36 turbine models provided valuable insights into optimal options tailored to each region's resources. Leading large-scale models like Suzlon's 4.0 MW S146 and MingYang's 3.0 MW MySE3.0-135 emerged as top performers consistently activating the highest numbers of concurrent EV charging ports. SANY's 2.0 MW SE12520 and Dongfang's 1.5 MW G2000-116 also demonstrated strong and stable port activations depending on site conditions. By characterizing regional wind patterns and identifying turbines, well-matched to local wind speeds, this study offers key information for decision-makers to maximize the potential contribution of onshore wind power resources towards Saudi Arabia's renewable energy and electrified transportation goals. Ongoing assessments and techno-economic analyses can further optimize project planning and rollout in suitable coastal territories.

ACKNOWLEDGMENT

Authors would like to acknowledge the technical support provided by King Fahd University of Petroleum & Minerals to accomplish the research work reported in this manuscript.

Nomenclature

BSS	Battery Storage System
c	Weibull Scale Parameter (m/s)
c_0	Scale Parameter at reference elevation z_0
CF	Capacity Factor
DC	Direct Current
E	Wind Energy (MWh)
EML	Empirical Method of Lysen
EMJ	Empirical Method of Justus
EV	Electrical Vehicle
HVAC	Heating Ventilation & Air Conditioning (HVAC)
GM	Graphical Method
IQR	Interquartile Range
k	Weibull Shape Parameter
k_0	Shape Parameter at reference elevation z_0
kW	Kilowatt
MLM	Maximum Likelihood Method
MM	Moment Method
MMLM	Modified Maximum Likelihood Method
MW	Megawatt
MWh	Megawatt Hour
N	Number of Charging Ports
P_d	Wind Power Density (W/m^2)
$P_{d,rated}$	Wind Power Density at Rated Speed (W/m^2)
$P_{d,output}$	Output Wind Power Density (W/m^2)
PDM	Power Density Method
t	Time Period
V	Wind Speed (m/s)
$V_{cut\ in}$	Cut in Speed (m/s)
$V_{cut\ out}$	Cut out Speed (m/s)
V_{rated}	Rated Speed (m/s)
V_m	Mean Wind Speed (m/s)
V_{fmax}	Most Frequently Occurring Wind Speed (m/s)
V_{Emax}	Maximum Energy Carrying Wind Speed (m/s)
W	Watt
Z	Hub height (m)

Greek symbols

ρ	Air Density (kg/m^3)
σ	Standard Deviation

REFERENCES

[1] Leung, J.Y.S., Russell, B.D., and Connell, S.D.: (2019) AR5 Synthesis Report: Climate Change 2014. One Earth Vol. 1, pp. 374–381, 2014.

[2] Krishnan, M., Samandari, H., Woetzel, J., et al.: The net-zero transition: What it would cost, what it could bring. McKinsey Co 1–64, 2022.

[3] GWEC (2023) Global Wind Report 2023

[4] Anonymous (2022) Saudi Energy Ministry plans pre-qualification for Yanbu wind project by Q3: MEED Arab News. https://www.arabnews.com/node/2072766/spa/aggregate. Accessed 3 Jan 2024

[5] Rašuo, B., Bengin, A., and Veg, A.: On Aerodynamic Optimization of Wind Farm Layout, PAMM Proc. Appl. Math. Mech., Vol. 10, No. 1, pp. 539–540, 2010. doi: 10.1002/pamm.201010262

[6] Mohandes, M., Khan, S.A., Rehman, S., Al-Shaikhi A., Liu, B., and Iqbal, K.: GARM: A Stochastic Evolution based Genetic Algorithm with Rewarding Mechanism for Wind Farm Layout Optimization, FME Transactions, Vol. 51, No. 4, 575-584, 2023.

[7] Rašuo, B., Dinulović, M., Veg, A., Grbović, A., Bengin, A.: Harmonization of new wind turbine rotor blades development process: A review, Renew. Sustain. Energy Rev., Vol. 39, pp. 874–882, 2014. doi: 10.1016/j.rser.2014.07.137

[8] Rehman, S., Baseer, M.A., and Alhems, L.M.: GIS-based multi-criteria wind farm site selection methodology, FME Transactions Vol. 48, No. 4, 855-867, 2020.

[9] Rašuo, B. P. and Bengin, A.: Optimization of wind farm layout, FME Transactions., Vol. 38, No. 3, pp. 107–114, 2010.

[10] Rehman, S., Natarajan, N., Mohandes, M.A., and Alam, M.M.: Latitudinal wind power resource assessment along coastal areas of Tamil Nadu, India, FME Transactions Vol. 48, 566-575, 2020.

[11] Dinulović, M.R., Trninić, M.R., Rašuo, B.P., and Kožović, D.V.: Methodology for aero-acoustic noise analysis of 3-bladed h-Darrieus wind turbine, Thermal Science, Vol. 27 (1 Part A), pp. 61-69, 2023. https://doi.org/10.2298/TSCI2301061D

[12] Rehman S., Kha S.A., and Alhems, L.M.: The Effect of Acceleration Coefficients in Particle Swarm Optimization Algorithm with Application to Wind Farm Layout Design, FME Transactions Vol. 48, No. (4), 922-930, 2020.

[13] Rašuo, B.P., and Veg, A.D.: Design, fabrication, and verification testing of the wind turbine rotor blades from composite materials, in: Proceedings of the ICCM-16, Japan, 2007, pp. 1-4.

[14] Ayodele, T.R., Jimoh, A.A., Munda, J.L., and Agee, J.T.: Viability and economic analysis of wind energy resource for power generation in Johannesburg, South Africa. Int J Sustain Energy Vol. 33, pp. 284–303, 2014. https://doi.org/10.1080/14786451.2012.762777

[15] Azad, K., Rasul, M., Halder, P., and Sutariya, J.: Assessment of wind energy prospect by weibull distribution for prospective wind sites in Australia. Energy Procedia Vol. 160, pp. 348–355, 2019. https://doi.org/10.1016/j.egypro.2019.02.167

[16] Aslam, M.: Testing average wind speed using sampling plan for Weibull distribution under indeterminacy. Sci Rep. Vol. 11, 2021. https://doi.org/10.1038/s41598-021-87136-8

[17] Jabbar, R.I.: Statistical Analysis of Wind Speed Data and Assessment of Wind Power Density Using Weibull Distribution Function (Case Study: Four Regions in Iraq). J Phys Conf Ser Vol. 1804, 2021. https://doi.org/10.1088/1742-6596/1804/1/012010

[18] Wan, J., Zheng, F., Luan, H., et al.: Assessment of wind energy resources in the urat area using optimized weibull distribution. Sustain Energy Technol Assessments Vol. 47, 2021. https://doi.org/10.1016/j.seta.2021.101351

[19] Kaplan, Y.A.: Calculation of Weibull distribution parameters at low wind speed and performance analysis. Proc Inst Civ Eng Energy Vol. 175, pp. 195–204, 2022. https://doi.org/10.1680/jener.21.00010

[20] Singh, K.A., Khan, M.G.M., and Ahmed, M.R.: Wind Energy Resource Assessment for Cook Islands with Accurate Estimation of Weibull Parameters Using Frequentist and Bayesian Methods. IEEE Access Vol. 10, pp. 25935–25953, 2022. https://doi.org/10.1109/ACCESS.2022.3156933

[21] Parezanovic, V., Rašuo, B., and Adzic, M.: Design of airfoils for wind turbine blades. in: Proceedings of the French-Serbian European Summer University: Renewable Energy Sources and Environment-Multidisciplinary Aspect, pp. 195-200, 2006.

[22] Nuha, H., Balghonaim, A., Pahlevi, R.R., Rehman, S., and Mohandes, M.: Vertical Wind Speed Extrapolation Using Statistical Approaches, FME Transactions, Vol. 52, No. (1), pp. 78-89, 2024.

[23] Rašuo, B., Bengin, A., Dinulović, M., Grbović, A.: Development of new optimal adapttronic airfoils, using modern engineering software packages, Tehnika, vol. 79, iss. 3, pp. 305-321, 2024. doi: 10.5937/tehnika2403305R

[24] Ouahabi, M.H., Elkhachine, H., Benabdelouahab, F., and Khamlichi, A.: Comparative study of five different methods of adjustment by the Weibull model to determine the most accurate method of analyzing annual variations of wind energy in Tetouan - Morocco. Procedia Manuf Vol. 46, pp. 698–707, 2020. https://doi.org/10.1016/j.promfg.2020.03.099

[25] Mahmood, F.H., Resen, A.K., and Khamees, A.B.: Wind characteristic analysis based on Weibull distribution of Al-Salman site, Iraq. Energy Reports Vol. 6, pp. 79–87, 2020. https://doi.org/10.1016/j.egyr.2019.10.021

[26] Rehman, S., Halawani, T.O., Husain, T.: Weibull parameters for wind speed distribution in Saudi Arabia. Sol Energy Vol. 53, pp. 473–479, 1994. https://doi.org/10.1016/0038-092X(94)90126 -M

[27] Alfawzan, F., Alleman, J.E., and Rehmann, C.R.: Wind energy assessment for Neom city, Saudi Arabia. Energy Sci Eng Vol. 8, pp. 755–767, 2020. https://doi.org/10.1002/ese3.548

[28] Anonymous (2023) International - U.S. Energy Information Administration (EIA). https://www.eia.gov/international/analysis/country/SAU. Accessed 4 Jan 2024

[29] Webpage (2024) POWER | Data Access Viewer. https://power.larc.nasa.gov/data-access-viewer/. Accessed 4 Jan 2024

[30] Kaplan, Y.A.: Calculation of Weibull distribution parameters at low wind speed and performance analysis. Proc Inst Civ Eng Energy Vol. 175, pp. 195–204, 2022. https://doi.org/10.1680/jener.21.00010

[31] Justus, C.G. and Mikhail, A.: Height variation of wind speed and wind distributions statistics. Geophys Res Lett Vol. 3, pp. 261–264, 1976. https://doi.org/10.1029/GL003i005p00261

[32] Manwell, J.F., McGowan, J.G., and Rogers, A.L.: 2010, Wind Energy Explained: Theory, Design and Application

[33] Bryden, T.S., Hilton, G., Cruden, A., Holton, T.: El–ectric vehicle fast charging station usage and power requirements. Energy Vol. 152, pp. 322–332, 2018. https://doi.org/10.1016/J.ENERGY.2018.03. 149

ПРОЦЕНА ПОТЕНЦИЈАЛА КОПНЕНЕ ЕНЕРГИЈЕ ВЕТРА ЗА МАКСИМИЗИРАЊЕ ЕЛЕКТРИФИКАЦИЈЕ ТРАНСПОРТА ПОДРЖАНОГ ОБНОВЉИВОМ ЕНЕРГИЈОМ – ПРИМЕЊЕНО ДУЖ ОБАЛЕ ЦРВЕНОГ МОРА САУДИЈСКЕ АРАБИЈЕ

Ш.З. Шуца, М. Алотаиби, Ш. Рехман

Ова студија процењује потенцијал енергије ветра на копну дуж обале Црвеног мора у Саудијској

Арабији како би се информисало о стратешком планирању за електрификацију транспорта подржаног обновљивим изворима енергије. Девет локација, међусобно удаљених 120-240 км, одабрано је на основу десетогодишњих података о брзини ветра и анализирано. Идентификовани су различити обрасци ветра између северозападне и југозападне обале. Добијени су метеоролошки подаци по сату (од јануара 2014. до децембра 2023. године) и процењене средње годишње вредности брзине ветра и густине снаге. Локације су процењене коришћењем НРЕЛ-овог система класификације. Студија је користила процену максималне вероватноће изведене из Вејбулове дистрибуције, облика и параметара размере за моделирање густине снаге и средње брзине. Фактори капацитета су анализирани за 36 модела ветротурбина снаге 1,5-4МВ да би се идентификовала ветротурбина која је оптимално прилагођена ресурсима ветра у сваком региону. Годишњи учинак фактора капацитета одредио је способност модела да поуздано активирају истовремене прикључке за пуњење електричних возила. Водећи избори укључивали су Сузлонов 4МВ С146 који доследно показује највећу средњу активацију порта. МингИанг-ов 3МВ МиСЕ3.0-135 и Виндеи-јев 3МВ ВД140-3000 су се показали као оптимални са стабилним двоцифреним активацијама портова у зависности од ресурса ветра. САНИ-јев 2МВ СЕ12520 и Виндеи-јев 2МВ ВД121-2000 такође су били истакнути на свим локацијама. Донгфанг Г2000-116 од 1,5 МВ задржао је јаке перформансе. Резултати карактеришу потенцијал енергије ветра и одређују оптималне изборе турбина које су способне да стабилно подрже циљеве електрификације транспорта у зависности од услова на локацији. Поред тога, резултати такође пружају вредне информације у вези са стратешким планирањем интеграције како би се максимизирао допринос копненог сектора ветра обновљивим изворима енергије и циљевима смањења емисија у Саудијској Арабији путем електрификованог транспорта.